Acta Biochim Biophys Sin, 2015, 47(12), 1023–1028
doi: 10.1093/abbs/gmv105
Advance Access Publication Date: 28 October 2015
Short Communication

Short Communication

A novel 4/6-type alpha-conotoxin VilA selectively inhibits nAchR α3β2 subtype

Liang Li[1,2,†], Na Liu[2,†], Rong Ding[2], Shuo Wang[2], Zhuguo Liu[2], Haiying Li[2], Xing Zheng[1], and Qiuyun Dai[2,*]

[1]Institute of Pharmacy and Pharmacology, University of South China, Hengyang 421001, China, and [2]Beijing Institute of Biotechnology, Beijing 100071, China

[†]These authors contributed equally to this work.
*Correspondence address. Tel: +86-10-66948897; Fax: +86-10-63833521; E-mail: qy_dai@yahoo.com

Received 2 February 2015; Accepted 24 August 2015

Abstract

Conotoxins (CTxs) are typically small peptides composed of 12–50 amino acid residues with 2–5 disulfide bridges. Most of them potently and selectively target a wide variety of ion channels and membrane receptors. They are highly valued as neuropharmacological probes and in pharmaceutical development. In this work, a novel α4/6-CTx named VilA (RDCCSNPPCAHNNPDC-NH_2) was identified from a cDNA library of the venom ducts of *Conus virgo* (*C. virgo*). VilA was then synthesized chemically and its disulfide connectivity was identified as 'C^1-C^3, C^2-$C^{4'}$. Its molecular targets were further assessed using two-electrode voltage clamping. The results indicated that VilA selectively inhibited nicotinic acetylcholine receptor (nAChR) α3β2 subtype with an IC_{50} of 845.5 nM, but did not target dorsal root ganglion sodium (Na^+)-, potassium (K^+)- or calcium (Ca^{2+})-ion channels. Further structure-activity relationship analysis demonstrated that Arg^1 and His^{11} but not Asp^2 were the functional residues. To the best of our knowledge, VilA is the first 4/6 α-CTx that selectively inhibits nAChR α3β2 subtype. This finding expands the knowledge of targets of α4/6-family CTxs.

Key words: α-conotoxin, VilA, cloning, synthesis, α3β2 nAChR subtype

Introduction

Conotoxins (CTxs), the small neurotoxic peptides composed of 12–50 amino acid residues with 2–5 disulfide bridges, are derived from the venom glands of cone snails. Based on the number of cysteine (C) residues, the arrangement of the disulfide bonds (S-Ss) and the consensus signal sequences, CTxs are categorized into various super-families (A, B, C, D, E, I, M, O, P, S and T etc.) [1,2]. To date, more than 26 super-families have been identified [1,2]. Most of them potently and selectively target a wide variety of ion channels, including sodium (Na^+)-, potassium (K^+)- and calcium Ca^{2+})-channels, as well as membrane receptors, including nicotinic acetylcholine receptor (nAChR), 5-hydroxytryptamine receptor (5-HT3R), N-methyl-D-aspartate receptor (NMDAR) and G-protein-coupled receptor (GPCR). They are highly valued as neuropharmacological probes and in pharmaceutical development [3–6].

Alpha-CTxs (α-CTxs) belong to the A-superfamily of CTxs and selectively inhibit nAChRs. Their sizes are typically in the range of 12–18 amino acid residues, including four C residues, CC-C-C, connected via the intra-chain -S-S- bridges in the 'C^1-C^3 and C^2-$C^{4'}$ arrangements [7]. According to the residue numbers of the inter cysteine loops [-CC-(loop1)-C-(loop2)-C-], they are further divided into several subfamilies (such as α3/5, α4/3, α4/4, α4/6, α4/7 and α5/5) [8–10]. For example, α3/5 CTxs mainly inhibit vertebrate muscular nAChRs, while α4/7 CTxs primarily target the vertebrate neuronal nAChRs [7,11]. To date, more than one hundred α-CTxs have been identified by direct peptide separation and gene cloning, of which, α4/7 CTxs are the most common ones. Only four α-CTxs belonging to 4/6 subgroup, including TxID, AuIB, Bu22 and TiIA, have been reported. TxID and AuIB are the inhibitors specific for α3β4 subtype [12–16]. However, Bu22 and TiIA have not been characterized

functionally yet. Moreover, some CTxs such as Vc1.1 and AuIB have been found to possess potent analgesic activity [17,18].

In this paper, we described the discovery, synthesis and functional characterization of a novel α4/6 CTx named ViIA which was identified from the worm-hunting cone snail, *Conus virgo* (*C. virgo*). Electrophysiological experiments showed that ViIA selectively inhibited the α3β2 subtype of nAChRs, but did not inhibit other subtypes including α2β2, α2β4, α3β4, α4β2, α4β4, α7 and α9α10. The key residues responsible for its effects on α3β2 subtype were further investigated. To the best of our knowledge, this is the first 4/6 type α-CTx that specifically inhibits α3β2 subtype. Therefore, this finding expands the scope of the α4/6 CTx family and the knowledge of the targets of α4/6-family CTx. This novel α-CTx will serve as a valuable neuropharmacological probe.

Materials and Methods

Reagents

N-Fmoc-amino acids and hydroxybenzotriazole (HOBt) were obtained from GL Biochem Ltd. (Shanghai, China). Rink resin was purchased from Tianjing Nankai Hecheng S&T Co. (Tianjin, China). N,N′-dicyclohexylcarbodiimide (DCC) and methanol were obtained from J&K Chemical LTD (Beijing, China) and Honeywell Burdick & Jackson (Muskegon, USA), respectively. The other reagents were of analytical grade.

Cloning of ViIA cDNA

ViIA was identified from the cDNA library of the venom ducts of *C. virgo* which was collected from the Xisha Island of the South China Sea. The cDNA library was constructed as reported previously [19,20]. Clones from the cDNA library were randomly picked and cultured in LB medium containing 100 μg/ml ampicillin. After being cultured, the clones were sequenced using the M13 forward primer. All the sequences were manually edited to discard vector and adaptor regions. The predicted protein sequences were analyzed using Seqtools (http://www.bio-soft.net/sms). The signal peptide sequences of the novel CTx precursors were predicted using the SignalP 3.0 Server (http://www.cbs.dtu.dk/services/SignalP/) [21]. A novel cDNA sequence of ViIA was identified by comparison with the sequences available in the GenBank nucleotide sequence database and in the literature, and was deposited in the Genbank nucleotide sequence database.

Peptide synthesis and *in vitro* folding

ViIA, its mutants and the control peptide RegIIA were synthesized using the method described previously [22,23]. Briefly, ViIA was assembled and then cleaved from Rink resin by treatment with the cleavage solution composed of 8.8 ml of trifluoroacetic acid (TFA), 0.5 ml of water, 0.5 g of dithiothreitol (DTT) and 0.2 ml of Triisopropylsilane. The released peptides (0.1 mg/ml) were oxidized in 0.1 M NH_4HCO_3 at room temperature, pH8.0–8.2. The folding products were then purified by semi-preparative reversed phase HPLC (RP-HPLC). The final products were assessed by analytical RP-HPLC. The primary sequence of ViIA is listed in Table 1.

Disulfide connectivity analysis

The disulfide bridge arrangement of the one-step oxidative folding product, α-ViIA, was determined by comparing the folded peptide products with the known disulfide connectivity [23]. The linear peptide containing an acetamidomethyl (Acm)-protecting group at the C^2-C^4 or C^1-C^4 position was folded by incubation in 0.1 M NH_4HCO_3 (pH 8.0) at room temperature for 24–48 h. The folded product was further oxidized with an iodine mixture containing 30% CH_3CN/2% TFA/68% H_2O for 10 min to yield a peptide with the -S-S- bridges of 'C^1-C^3, C^2-C^4' or 'C^1-C^4, C^2-C^3'. This second oxidized product was co-applied with the one-step folding product, ViIA, to determine the disulfide connectivity.

Circular dichroism (CD) spectra

CD spectra of ViIA were measured between 190 and 340 nm on a Bio-Logic Mos 450 spectropolarimeter (Biologic, Grenoble, France). The ViIA peptide was dissolved in 0.01 M phosphate buffer (pH 7.2) to a

Table 1. Amino acid sequences of some α-CTxs targets nAChR α3β2 or α3β4

αm/n	Peptide	Sequence	nAChR subtypes (IC_{50}, nM)	Reference
α4/6	ViIA	RDCCSNPPCAHNNPD-C[a]	α3β2 (848.5)	This work
	TxID	GCCSHPVCSAMSPI-C[a]	α3β4 (12.5) > α6/α3β4 (94) > α2β4 (4550)	[12]
	AuIB	GCCSYPPCFATNPD-C[a]	α3β4 (750) > α7	[14]
	Bu22	GCCTYPPCAVLSPL-CD	N.D.	[15]
	TiIA	GGCCSHPACQNNPDy-C[a]	N.D.	[16]
α4/7	ArIA	IRDECCSNPACRVNNOHVCRRR	α3β2 (18) < α7 (6.02)	[24]
	AnIB	GGCCSHPACAANNQDYC[a]	α3β2 (0.3) > α7 (76)	[25]
	GIC	GCCSHPACAGNNQHIC[a]	α3β2 (1.1) > α4β2 (309) > α3β4 (755)	[26]
	GID	IRDγCCSNPACRVNNOHVC	α3β2 (3.4) ≈ α7 (5.1) > α4β2 (128.6)	[19]
	LsIA	SGCCSNPACRVNNPNIC[a]	α3β2 (10.3) ≈ α7 (10.1)	[27]
	MII	GCCSNPVCHLEHSNLC[a]	α3β2 (2.20) ≈ α6/α3β2β3 (0.39)	[28]
	OmIA	GCCSHPACNVNNPHICG[a]	α3β2 (11) > α7 > α6/α3β2β3 (201)	[29]
	PeIA	GCCSHPACSVNHPELC[a]	α9α10 (6.9) > α3β2 (23) > α3β4 (480) > α7 (1800)	[30]
	PnIA	GCCSLPPCAANNPDYC[a]	α3β2 (9.6) > α7 (252)	[31]
	RegIIA	GCCSHPACNVNNPHIC[a]	α3β2 (33) > α3β4 (97) > α7 (103) > α9α10 (>1000)	[32]
	TxIA	GCCSRPPCIANNPDLC[a]	α3β2 (3.6) > α7 (392)	[33]
	Vc1.1	GCCSDPRCNYDHPEIC[a]	α9α10 > α6/α3β2β3 > α6/α3β4 > α3β4 > α3β2	[34]
α4/3	ImI	GCCSDPRCAWR----C[a]	α3β2 (41) > α7 (595) > α9α10 (2000)	[35]

ViIA is the new peptide identified in this work; αm/n denote α-CTxs subgroups (4/6, 4/7 and 4/3); Amino acid conservations are denoted by light gray shade.
[a]Denote the C-terminal amide; N.D.: untested.

```
1   ATG GGC ATG CGG ATG ATG TTC GTC GTG TTT CTG TTG GTT GTC TTC GCA TCC TCT GTC ACC   60
1   M   G   M   R   M   M   F   V   V   F   L   L   V   V   F   A   S   S   V   T    20
61  TTA GAT CGT GCA TCT TAT GGC AGG TAT GCT TCA CCC GTC GAC AGA GCG TCT GCC CTG ATC  120
21  L   D   R   A   S   Y   G   R   Y   A   S   P   V   D   R   A   S   A   L   I    40
121 GCT CAG GCC ATC CTT CGA GAT TGC TGC TCC AAT CCT CCT TGT GCC CAT AAT AAT CCA GAC  180
41  A   Q   A   I   L   R   D   C   C   S   N   P   P   C   A   H   N   N   P   D    60
181 TGT CGT TAA                                                                    189
61  C   R   *
```

Figure 1. The cDNA sequence and predicted translation product of VilA The signal peptide and mature toxin are shaded. The codons of conserved Cys are shown in bold letter. The nucleotide sequence data are available in the GenBank database under the accession numbers JF436964.1 for VilA.

final concentration of 35 μM. A 1-cm path length quartz cell was employed. Each spectrum represents the accumulation of eight individual scans collected at 1.0 nm intervals at a bandwidth of 1.0 nm.

Two-electrode voltage-clamp recording on oocytes

cDNA preparation, oocytes harvest and expression of nAChR subunits were performed as described previously with some modifications [23,24]. Each *Xenopus* oocyte was injected with at least 20 ng of cDNA and incubated with ND96 solution (96.0 mM NaCl, 2.0 mM KCl, 1.8 mM $CaCl_2$, 1.0 mM $MgCl_2$ and 5 mM HEPES, pH 7.3) containing 2.5 mM pyruvic acid sodium and mixed antibiotics of 100 U/ml penicillin and 100 μg/ml streptomycin (Sigma, St Louis, USA) at 18°C. Data were recorded at days 2–5 post-injection at room temperature.

The oocytes were gravity-perfused in a recording chamber (50 μl) with ND96 at a rate of 1.5 ml/min. The membrane potential was clamped at −70 mV and the ACh-gated currents were recorded with a two-electrode voltage-clamp amplifier Axoclamp 900A (Axon Instruments Inc., Union City, USA). To measure the baseline responses, the oocytes were continuously perfused with ND96, during which ACh was automatically applied at a 5-min interval. To measure the dose-dependent response, the oocytes were continuously perfused with toxin solution until equilibrium (5–10 min) prior to the ACh pulse. AChs were prepared with ND96 at concentrations of 200 μM for α7, 30 μM for α9α10 and 100 μM for the others, respectively. The concentration of stock solution of peptide in water was determined by the HPLC method according to the protocol of Proteins & Peptides A205 with the Thermo Scientific NanoDrop 2000/2000c spectrophotometer [36], and then diluted with 0.1 mg/ml BSA to reduce the non-specific adsorption.

The dose-dependent response data were fit to the equation: response (%) = $100/[1 + ([\text{toxin}]/IC_{50})^n]$, where n is the Hill coefficient and IC_{50} is the antagonist concentration giving half-maximal response, by non-linear regression analysis using GraphPad Prism (GraphPad Software, San Diego, USA).

Results

The identification of a novel α-CTx VilA

A novel CTx precursor was isolated from a cDNA library of *C. virgo*. The mature toxin sequence was predicted as RDCCSNPPCAHNNPDC-NH_2 with a cysteine (C) pattern of CCX_4CX_6C (X represents any other amino acids), suggesting that this peptide belongs to the α4/6 family CTx. In accordance with conventional CTx nomenclature, the cloned sequence that encodes the novel CTx was designated as VilA. This cDNA sequence has been submitted to GenBank and its GenBank accession number is JF436964.1 (**Fig. 1**).

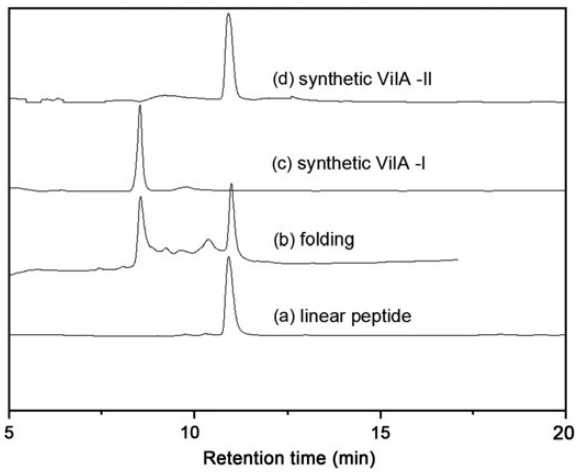

Figure 2. HPLC analysis of the folded products of linearized VilA One-step oxidative folding of VilA. Traces from bottom to top: (a) The linearized peptide; (b) One-step oxidized products; (c) The purified product of VilA-I; (d) The purified product of VilA-II. Samples were applied to a Calesil ODS-100 C18 column (4.6 mm × 250 mm) and eluted with a linear gradient of 5%–10% B for 0–1 min; 10%–50% B for 25 min and 50%–95% B for 25–28 min at flow rate of 1 ml/min, the eluted peptides were monitored at 214 nm. B is acetonitrile in 0.1% TFA.

Peptide synthesis and disulfide connectivity in VilA

HPLC results of the one-step and two-step folding of the two different AcmAcm-protected VilA linear peptides are shown in **Figs. 2 and 3**. Two major peaks, VilA-I and VilA-II, were the two-bridge isomers formed during oxidative folding of the linear peptide, respectively (**Fig. 2**). The folding conditions [(i) 0.1 M NH_4HCO_3, pH 8.1; (ii) 0.1 M NH_4Ac, pH 8.1; (iii) 0.1 M NH_4HCO_3 + 1 M $(NH_4)_2CO_3$, pH 8.1; (iv) 0.1 M Tris·HCl, pH 8.1 and (v) 0.1 M Tris·HCl + 1 mM GSH + 0.1 mM GSSG, pH 8.1)] did not significantly affect the ratio of

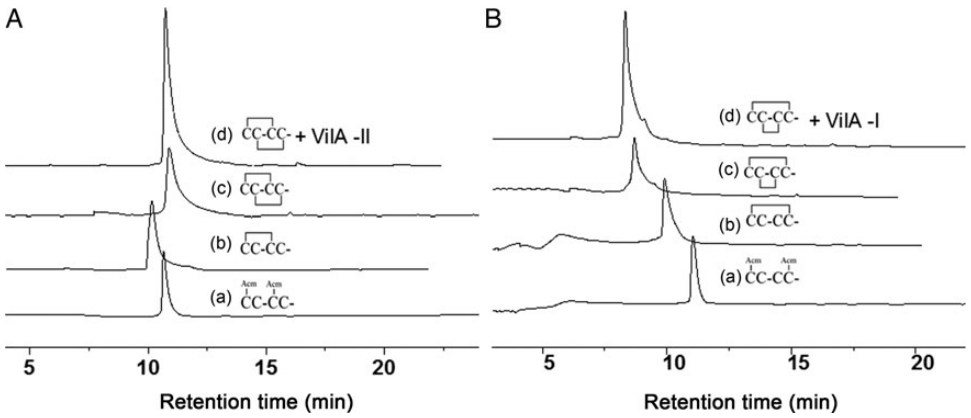

Figure 3. HPLC analysis of the folded products of linear VilA with Acm modification (A) Determination of the disulfide bond connectivity of VilA-II. Traces from bottom to top: (a) Linear peptide with Acm modifications at Cys1 and Cys3; (b) the first oxidized product; (c) The second oxidized product and (d) co-elution of the two-step folding products and the purified product VilA-II. (B) Determination of disulfide bond connectivity of VilA-I: Traces from bottom to top: (a) Linear peptide with Acm modifications at Cys1 and Cys4; (b) The first oxidized product; (c) The second oxidized product; (d) Co-elution of the two-step folding products and the purified product VilA-I. Analytical conditions were the same as those described in **Fig. 2**.

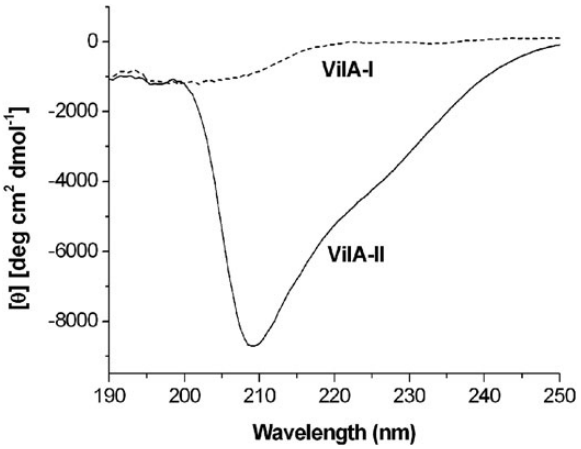

Figure 4. CD spectra of VilA in 0.01 M phosphate buffer solution The peptides were dissolved in 0.01 M phosphate buffer (pH 7.2) to a final concentration of 35 μM. A 1 cm path length quartz cell was employed. Each spectrum represents the accumulation of eight individual scans collected at 1.0 nm intervals at a bandwidth of 1.0 nm.

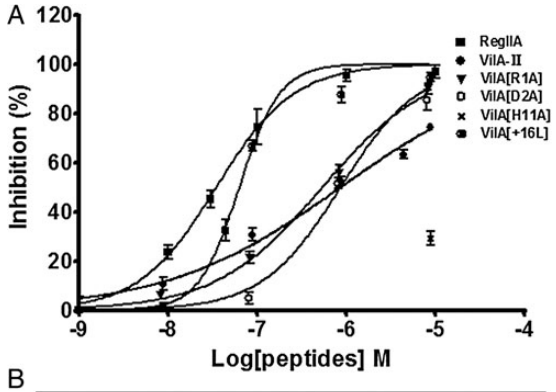

B

Peptides	IC_{50}(α3β2,nM)
RegIIA	34.5(26.0-45.7)
VilA-I	>10000
VilA-II	848.5(596.5-1207.0)
VilA[R1A]	532.4(428.5-661.5)
VilA[D2A]	854.1(655.1-1113.5)
VilA[H11A]	>10000
VilA[+16L]	62.6(54.8-71.5)

Figure 5. Effects of VilA on rat nAChRs expressed in *Xenopus* oocytes (A) Concentration-dependent response curves of the rat α3β2 nAChR (n = 4–6). (B) IC_{50} of peptides on various rat nAChR subtypes. The control peptide for α3β2 was RegIIA (IC_{50} = 34.5 nM). Peptides were applied by perfusion to oocytes expressing AChRs as described in Materials and Methods. Numbers in parentheses indicate 95% confidence intervals. VilA was tested on α7, α3β4, α4β2, α2β2, α2β4, α9α10 and α4β4 nAchR subtypes with the IC_{50} > 10 μM.

ViIA-I/ViIA-II (**Supplementary Fig. S1**). Mass spectral analysis with Bruker Ultraflex III TOF/TOF mass spectrometry (Bruker, Billerica, USA) showed that the molecular weights are the same as those expected. For example, the monoisotopic m/zs for ViIA-I and Vil.6-II were 1740.6549 and 1740.6157, respectively, which were almost identical to the calculated m/z (1740.6407). A co-elution assay performed with ViIA-I, Vil.6-II and the two products formed in the two-step oxidative folding reaction indicated that ViIA-II has a disulfide connectivity arrangement of 'C^1-C^3, C^2-C^4' (**Fig. 3A**) and the ViIA-I has the arrangement of 'C^1-C^4, C^2-C^3'(**Fig. 3B**).

The ViIA variants were also synthesized as described above and assessed by analytical RP-HPLC. Their purities were >98% with the expected molecular weights.

CD spectra of VilA

The CD spectra of ViIA-II in 0.01 M phosphate buffer (pH 7.2) showed some ellipticities around 208 nm and 220 nm (**Fig. 4**), indicating that it has a helical structure. However, ViIA-I did not show any significant helical folding.

Activities of VilA and its variants on nAChRs

Two-electrode voltage clamping was used to assess the effects of ViIA and its variants on various neuronal nAChRs expressed by *Xenopus* oocytes. As shown in **Fig. 5**, ViIA-II exhibited an inhibition on the rat neuronal subtype α3β2 with an IC_{50} of 845.5 nM, but not on the subtypes of α2β2, α2β4, α3β4, α4β2, α4β4, α7 or α9α10 (IC_{50} > 10 μM).

These results indicate that ViIA-II selectively inhibits the α3β2 subtype of nAChRs. However, ViIA-I having the disulfide connectivity arrangements of 'C^1-C^4, C^2-C^3' displayed no apparent inhibitory effects on nAChR subtypes with the inhibitory ratio lower than 15% at 10 μM. When His^{11} was mutated to Ala, the binding ratio was decreased to lower than 50% at 10 μM. On the contrary, the substitution of Arg^1 with Ala resulted in an increase in inhibitory activity on α3β2 with an IC_{50} of 532.4 nM (428.5–661.5 nM). Interestingly, ViIA(+16L), in which a Leu residue was added ahead of the last Cys, displayed a significantly elevated binding activity with an IC_{50} of 62.6 nM.

Discussion

Up till now, four α4/6-CTxs, including TxID, AuIB, Bu22 and TiIA, have been reported (Table 1). Both TxID and AuIB were shown to be the specific inhibitors of α3β4 subtype [12–14], but Bu22 and TiIA have not been characterized functionally [15,16]. In this study, we identified and characterized a novel α4/6 CTx known as ViIA and found that it specifically inhibited the α3β2 subtype but did not display any inhibitory effects on the subtypes of α2β2, α2β4, α3β4, α4β2, α4β4, α7 or α9α10 (IC_{50} > 10 μM). In addition, ViIA had no significant effect on dorsal root ganglion (DRG) Na^+-, K^+- or Ca^{2+}-channels (data not shown). To the best of our knowledge, ViIA is the first α4/6 -CTx that inhibits the nAChR α3β2 subtype. The target preference of ViIA may be attributed to its unique sequence because sequence alignment reveals that ViIA shares 55%, 69%, 75% and 75% sequence identity with those of TxID, TiIA, AuIB and Bu22, respectively.

Currently, several α-CTx subtypes, including 4/3, 4/4, 4/5 and 4/7 subtypes, have been found to potently inhibit the α3β2 nAChR subtype (Table 1) [24–35]. However, they also inhibit other nAChR subtypes, such as α7, α9 α10, α2β4 and α3β4. On the contrary, ViIA selectively inhibits the α3β2 subtype though its IC_{50} is not very high. Compared with other α-CTxs targeting the α3β2 subtype [37,38], ViIA displays a low content of helical conformation (**Fig. 4**). The unique residues at its N-terminal and in loop 2 may mainly contribute to its high selectivity.

It should be noted that there are a basic (Arg) residue and an acidic (Asp) residue upstream of the first cysteine (C) residue. This phenomenon rarely occurs in other α-CTxs targeting the α3β2 subtype. To investigate the contributions of the two residues, we synthesized two mutants. The replacement of Asp^2 by Ala in ViIA did not decrease the activity (IC_{50} = 854.1 nM), but the substitution of Arg^1 with Ala led to an increase in the activity (IC_{50} = 532.4 nM). Based on the structure-activity information of α-CTxs targeting the α3β2 subtype [13,30], His^{11} of ViIA was selected to be mutated. The result showed that the replacement of His^{11} by Ala resulted in a sharp decrease in the activity (IC_{50} < 10 μM). These results suggest that both Arg^1 and His^{11} are the crucial residues.

Based on the sequence identity between the 4/7 α-CTxs and ViIA at position 16 (Table 1) [25–34], a mutant ViIA[+16L] (RDCCSNPPCAHNNPDLC-NH_2) was synthesized and functionally characterized. The results showed that ViIA[+16L] exhibited 12-folds higher binding ability than ViIA, with an IC_{50} of 62.6 nM. It is likely due to the fact that Leu residue may increase the hydrophobicity of this peptide. This is consistent with a previous report that the hydrophobic residue at position 16 is important for its inhibitory activity towards the α3β2 nAChR subtype [39].

Two major peaks (ViIA-I and ViIA-II) existed during the oxidative folding reaction of the linear ViIA peptide. Further activity assay demonstrated that ViIA-II, which has the disulfide connectivity of 'C^1-C^3 and C^2-C^4', displayed a strong binding ability to the α3β2 nAChR subtype. However, ViIA-I, which has the disulfide connectivity of 'C^1-C^4, C^2-C^3', did not bind to α3β2 or other nAChR subtypes, suggesting that ViIA-II may be the natural peptide, though it has not been reported in the venom.

In conclusion, we found a novel α4/6 CTx ViIA targeting specifically the α3β2 nAChR subtype. This finding expands our knowledge about the target of the CTxs in α4/6 family and provides a motif for designing novel inhibitors specifically for the α3β2 nAChR subtype.

Supplementary Data

Supplementary data is available at *ABBS* online.

Acknowledgements

We would like to thank Professor Jiuping Ding from College of Life Science and Technology, Huazhong University of Science and Technology (Wuhan, China), for his help in the binding assay of ViIA in rat DRG cells.

Funding

This work was supported by the grants from the National Natural Science Foundation of China (No. 81173035), the National Basic Research Program of China (No. 2010CB529802) and the National High Technology and Development Program of China (No. SS2013AA090204).

References

1. Robinson SD, Norton RS. Conotoxin gene superfamilies. *Mar Drugs* 2014, 12: 6058–6101.
2. Akondi KB, Muttenthaler M, Dutertre S, Kaas Q, Craik DJ, Lewis RJ, Alewood PF. Discovery, synthesis, and structure-activity relationships of conotoxins. *Chem Rev* 2014, 114: 5815–5847.
3. Lewis RJ, Dutertre S, Vetter I, Christie MJ. Conus venom peptide pharmacology. *Pharmacol Rev* 2012, 64: 259–298.
4. Adams DJ, Berecki G. Mechanisms of conotoxin inhibition of N-type (Ca(v)2.2)calcium channels. *Biochim Biophys Acta* 2013, 1828: 1619–1628.
5. Prorok M, Castellino FJ. The molecular basis of conantokin antagonism of NMDA receptor function. *Curr Drug Targets* 2007, 8: 633–642.
6. Terlau H, Olivera BM. Conus venoms: a rich source of novel ion channel-targeted peptides. *Physiol Rev* 2004, 84: 41–68.
7. Lebbe EK, Peigneur S, Wijesekara I, Tytgat J. Conotoxins targeting nicotinic acetylcholine receptors: an overview. *Mar Drugs* 2014, 12: 2970–3004.
8. Azam L, Mclntosh JM. Alpha-conotoxins as pharmacological probes of nicotinic acetylcholine receptors. *Acta Pharmacol Sin* 2009, 30: 771–783.
9. Peng C, Chen WH, Sanders T, Chew G, Liu J, Hawrot E, Chi CW. Chemical synthesis and characterization of two α4/7-conotoxins. *Acta Biochim Biophys Sin* 2010, 42: 745–753.
10. Lebbe EK, Peigneur S, Maiti M, Mille BG, Devi P, Ravichandran S, Lescrinier E, *et al*. Discovery of a new subclass of α-conotoxins in the venom of *Conus australis*. *Toxicon* 2014, 91: 145–154.
11. Liu L, Chew G, Hawrot E, Chi C, Wang C. Two potent alpha3/5 conotoxins from piscivorous *Conus achatinus*. *Acta Biochim Biophys Sin* 2007, 39: 438–444.
12. Luo S, Kulak JM, Cartier GE, Jacobsen RB, Yoshikami D, Olivera BM, McIntosh JM. Alpha-conotoxin AuIB selectively blocks alpha3 beta4 nicotinic acetylcholine receptors and nicotine evoked norepinephrine release. *J Neurosci* 1998, 18: 8571–8579.

13. Grishin AA, Cuny H, Hung A, Clark RJ, Brust A, Akondi K, Alewood PF, *et al*. Identifying key amino acid residues that affect α-conotoxin AuIB inhibition of α3β4 nicotinic acetylcholine receptors. *J Biol Chem* 2013, 288: 34428–34442.
14. Luo S, Zhangsun D, Zhu X, Wu Y, Hu Y, Christensen S, Harvey PJ, *et al*. Characterization of a novel α-conotoxin TxID from *Conus textile* that potently blocks rat α3β4 nicotinic acetylcholine receptors. *J Med Chem* 2013, 56: 9655–9663.
15. Hu H, Bandyopadhyay PK, Olivera BM, Yandell M. Characterization of the *Conus bullatus* genome and its venom-duct transcriptome. *BMC Genomics* 2011, 12: 60.
16. Kauferstein S, Porth C, Kendel Y, Wunder C, Nicke A, Kordis D, Favreau P, *et al*. Venomic study on cone snails (*Conus spp*.) from South Africa. *Toxicon* 2011, 57: 28–34.
17. Satkunanathan N, Livett B, Gayler K, Sandall D, Down J, Khalil Z. Alpha-conotoxin Vc1.1 alleviates neuropathic pain and accelerates functional recovery of injured neurons. *Brain Res* 2005, 1059: 149–158.
18. Napier IA, Klimis H, Rycroft BK, Jin AH, Alewood PF, Motin L, Adams DJ, *et al*. Intrathecal α-conotoxins Vc1.1, AuIB and MII acting on distinct nicotinic receptor subtypes reverse signs of neuropathic pain. *Neuropharmacology* 2012, 62: 2202–2207.
19. Conticello SG, Gilad Y, Avidan N, Ben-Asher E, Levy Z, Fainzilber M. Mechanisms for evolving hypervariability: the case of conopeptides. *Mol Biol Evol* 2001, 18: 120–131.
20. Liu Z, Li H, Liu N, Wu C, Jiang J, Yue J, Jing Y, *et al*. Diversity and evolution of conotoxins in *Conus virgo*, *Conus eburneus*, *Conus imperialis* and *Conus marmoreus* from the South China Sea. *Toxicon* 2012, 60: 982–989.
21. Bendtsen JD, Nielsen H, von Heijne G, Brunak S. Improved prediction of signal peptides: SignalP 3.0. *J Mol Biol* 2004, 340: 783–795.
22. Dai Q, Sheng Z, Geiger JH, Castellino FJ, Prorok M. Helix-helix interactions between homo- and heterodimeric gamma-carboxyglutamate-containing conantokin peptides and their derivatives. *J Biol Chem* 2007, 282: 12641–12649.
23. Wang S, Du T, Liu Z, Wang S, Wu Y, Ding J, Jiang L, *et al*. Characterization of a T-superfamily conotoxin TxVC from Conus textile that selectively targets neuronal nAChR subtypes. *Biochem Biophys Res Commun* 2014, 454: 151–156.
24. Whiteaker P, Christensen S, Yoshikami D, Dowell C, Watkins M, Gulyas J, Rivier J, *et al*. Discovery, synthesis, and structure activity of a highly selective alpha7 nicotinic acetylcholine receptor antagonist. *Biochemistry* 2007, 46: 6628–6638.
25. Loughnan ML, Nicke A, Jones A, Adams DJ, Alewood PF, Lewis RJ. Chemical and functional identification and characterization of novel sulfated alpha-conotoxins from the cone snail conus anemone. *J Med Chem* 2004, 47: 1234–1241.
26. McIntosh JM, Dowell C, Watkins M, Garrett JE, Yoshikami D, Olivera BM. Alpha-conotoxin GIC from *Conus geographus*, a novel peptide antagonist of nicotinic acetylcholine receptors. *J Biol Chem* 2002, 277: 33610–33615.
27. Inserra MC, Kompella SN, Vetter I, Brust A, Daly NL, Cuny H, Craik DJ, *et al*. Isolation and characterization of alpha-conotoxin lsia with potent activity at nicotinic acetylcholine receptors. *Biochem Pharmacol* 2013, 86: 791–799.
28. Cartier GE, Yoshikami D, Gray WR, Luo S, Olivera BM, McIntosh JM. A new alpha-conotoxin which targets alpha3beta2 nicotinic acetylcholine receptors. *J Biol Chem* 1996, 271: 7522–7528.
29. Chi SW, Kim DH, Olivera BM, McIntosh JM, Han KH. Solution conformation of a neuronal nicotinic acetylcholine receptor antagonist alpha-conotoxin OmIA that discriminates alpha3 vs, alpha6 nAChR subtypes. *Biochem Biophys Res Commun* 2006, 345: 248–254.
30. McIntosh JM, Plazas PV, Watkins M, Gomez-Casati ME, Olivera BM, Elgoyhen AB. A novel alpha-conotoxin, peia, cloned from conus pergrandis, discriminates between rat alpha9alpha10 and alpha7 nicotinic cholinergic receptors. *J Biol Chem* 2005, 280: 30107–30112.
31. Hopping G, Wang CI, Hogg RC, Nevin ST, Lewis RJ, Adams DJ, Alewood PF. Hydrophobic residues at position 10 of alpha-conotoxin pnia influence subtype selectivity between alpha7 and alpha3beta2 neuronal nicotinic acetylcholine receptors. *Biochem Pharmacol* 2014, 91: 534–542.
32. Franco A, Kompella SN, Akondi KB, Melaun C, Daly NL, Luetje CW, Alewood PF, *et al*. Regiia: An alpha4/7-conotoxin from the venom of *Conus regius* that potently blocks alpha3beta4 nachrs. *Biochem Pharmacol* 2012, 83: 419–426.
33. Dutertre S, Ulens C, Buttner R, Fish A, van Elk R, Kendel Y, Hopping G, *et al*. Achbp-targeted alpha-conotoxin correlates distinct binding orientations with nachr subtype selectivity. *EMBO J* 2007, 26: 3858–3867.
34. Halai R, Clark RJ, Nevin ST, Jensen JE, Adams DJ, Craik DJ. Scanning mutagenesis of alpha-conotoxin vc1.1 reveals residues crucial for activity at the alpha9alpha10 nicotinic acetylcholine receptor. *J Biol Chem* 2009, 284: 20275–20284.
35. Ellison M, Gao F, Wang HL, Sine SM, McIntosh JM, Olivera BM. Alpha-conotoxins ImI and ImII target distinct regions of the human alpha7 nicotinic acetylcholine receptor and distinguish human nicotinic receptor subtypes. *Biochemistry* 2004, 43: 16019–16026.
36. Scopes RK. Measurement of protein by spectrophotometry at 205nm. *Anal Biochem* 1974, 59: 277–282.
37. Lamthanh H, Jegou-Matheron C, Servent D, Ménez A, Lancelin JM. Minimal conformation of the alpha-conotoxin ImI for the alpha7 neuronal nicotinic acetylcholine receptor recognition: correlated CD, NMR and binding studies. *FEBS Lett* 1999, 454: 293–298.
38. Wang S, Zhao C, Liu Z, Wang X, Liu N, Du W, Dai Q. Structural and functional characterization of a novel α-conotoxin Mr1.7 from *Conus marmoreus* targeting neuronal nAChR α3β2, α9α10 and α6/α3β2β3 subtypes. *Mar Drugs* 2015, 13: 3259–3275.
39. Muttenthaler M, Akondi KB, Alewood PF. Structure-activity studies on alpha-conotoxins. *Curr Pharm Des* 2011, 17: 4226–4241.